AAPS PharmSciTech (2024) 25:192
https://doi.org/10.1208/s12249-024-02912-9

RESEARCH ARTICLE

Thermally-Induced Supersaturation Approach for Optimizing Drug Loading and Biopharmaceutical Properties of Supersaturated Lipid-Based Formulations: Case Studies with Ibrutinib and Enzalutamide

Arvind Sirvi[1] · Akash Janjal[1] · Kajal Guleria[1] · Mahesh Chand[1] · Abhay T. Sangamwar[1]

Received: 7 June 2024 / Accepted: 31 July 2024

Abstract
Lipid-based formulations (LbFs) have demonstrated success in pharmaceutical applications; however, challenges persist in dissolving entire doses of the drug into defined liquid volumes. In this study, the temperature-induced supersaturation method was employed in LbF to address drug loading and pill burden issues. Supersaturated LbFs (super-LbF) were prepared using the temperature-induced supersaturation method, where the drug load is above its equilibrium solubility. Further, the influence of the drug's physicochemical and thermal characteristics on drug loading and their relevance with an apparent degree of supersaturation (aDS) was studied using two model drugs, ibrutinib and enzalutamide. All the prepared LbFs were evaluated in terms of physical stability, dispersion, and solubilization capacity, as well as pharmacokinetic assessments. Drug re-crystallization was observed in the lipid solution on long-term storage at higher aDS values of 2–2.5. Furthermore, high-throughput lipolysis studies demonstrated a significant decrease in drug concentration across all LbFs (regardless of drug loading) due to a decline in the formulation solvation capacity and subsequent generation of *in-situ* supersaturation. Further, the *in vivo* results demonstrated comparable pharmacokinetic parameters between conventional LbF and super-LbF. The short duration of the thermodynamic metastable state limits the potential absorption benefits. However, super-LbFs of Ibr and Enz showed superior profiles, with 1.7-fold and 5.2-fold increased drug exposure compared to their respective crystalline suspensions. In summary, this study emphasizes the potential of temperature-induced supersaturation in LbF for enhancing drug loading and highlights the intricate interplay between drug properties, formulation characteristics, and *in vivo* performance.

Keywords aqueous solubilization · lipid-based formulation · oral absorption · physical stability · temperature-induced supersaturation

Introduction

In recent years, advancements in drug discovery technologies and methodologies, such as high-throughput screening and computational chemistry, have led to the identification of a growing number of lipophilic drug candidates with poor absorption profiles [1, 2]. Therefore, there is a need to develop an efficient formulation approach to enhance the absorption profile of these drugs. Particularly, lipid-based formulation (LbF) as a supersaturating formulation has gained significant attention for the oral delivery of drug molecules with limited solubility and dissolution-limited characteristics [3, 4]. This approach facilitates the direct delivery of drugs in a solution form to the gastric region, thereby bypassing the rate-limiting dissolution step [5]. In the literature, it has been demonstrated that LbF can enhance absorption while reducing the positive food effect and inter-subject variability [3]. Despite the aforementioned advantages, conventional LbFs are unable to accommodate higher drug loading due to the low oil solubility of drugs. This is particularly challenging in preclinical dose escalation studies, where higher oral

✉ Abhay T. Sangamwar
abhays@niper.ac.in; abhaysangamwar@gmail.com

[1] Department of Pharmaceutics, National Institute of Pharmaceutical Education and Research, Sector-67, S.A.S Nagar, Punjab 160062, India

Published online: 20 August 2024

doses of drugs are required [6]. Additional factors, such as drug precipitation during colloidal dispersions, physical instability, and inadequate *in vitro-in vivo* correlation, have been recognized as obstacles to fully realizing the therapeutic potential and commercial success of conventional LbFs [7].

Thus, significant advancements are ongoing in the field of LbFs, including the exploration of supersaturated LbF (super-LbF), intending to boost drug loading capacities and simultaneously reduce pill burden [8–12]. Super-LbF elevates the drug concentration above its equilibrium solubility in lipid solution by employing temperature-based or ionic liquid-based supersaturation [7, 8, 13, 14]. Among these methods, temperature-mediated supersaturation is a highly considered and feasible approach to elevate the drug solubility in the lipid solution. In this approach, supersaturation is induced directly in LbF thermally, by heating the lipid solution to, for example, 60–65°C, saturating the system with the drug, and subsequently cooling it down to ambient temperature. The apparent degree of supersaturation (aDS) is often used to express supersaturation terminology as well as define drug payload within LbF, represented in Eq. 1. Where C is the solubilized concentration in super-LbF and C* is its saturation solubility in particular lipid solution at ambient temperature [15].

$$\mathrm{aDS} = \frac{C}{C^*} \tag{1}$$

The aDS in LbF significantly influences critical quality attributes such as physical stability, dispersion capacity, aqueous solubilization, and subsequently *in vivo* absorption. To date, few studies have reported on the influence of aDS achieved through temperature-mediated supersaturation. Schultz *et al*. observed a linear correlation between processing temperature and increased solubility in lipidic vehicles [16]. Consistent with previous findings, Almasri *et al*. also reported a 4–sevenfold increase in fenofibrate solubility in medium-chain triglyceride-based oils when the processing temperature was set at 60°C compared to 25°C [17]. Due to the high degree of supersaturation, the physical stability of liquid LbF is of significant interest. Bannow *et al*. demonstrated that the increased thermodynamic driving force is responsible for drug re-crystallization within lipid solution due to the higher degree of supersaturation (aDS value of 2.5) and the onset of precipitation time was within 24 h [18]. Similarly, Ilie *et al*. also observed that high aDS values (> 1.35) trigger drug crystallization within the vehicle during 28 days of storage period. These observations were found to be more dependent on the type of drug rather than the type of lipid vehicle [19]. The physicochemical properties of drugs, such as lipophilicity, melting point, glass-forming ability, and propensity to supersaturate within a lipid vehicle affect their physical stability [8, 19]. Therefore, investigating the influence of drug properties is essential for designing super-LbF.

Biopharmaceutical assessment of super-LbF serves as a pivotal determinant that reflects their true potential for clinical success. To date, super-LbF are well explored for the selection of excipients or different types of LbF using *in vitro* dispersion and digestion settings. In the literature, it has been observed that super-LbF generates *in-situ* supersaturation in the non-sink digestive condition due to a reduction in solubilization capacity upon dispersion [4]. However, the rate and extent of supersaturation depend on several factors, including lipid excipients, drug payload, the nature of the drug, and interactions of the drug with solubilizing species in digestive conditions [5]. The imbalance of supersaturation in the intraluminal passage could affect the *in vivo* absorption of drugs, leading to variable outcomes, as evidenced in the literature [7]. Ilie *et al*. observed a noteworthy 2.3 to 2.5-fold increase in celecoxib exposure following the oral administration of type I based super-LbF compared to non-supersaturated LbF formulations, attributed to the enhanced supersaturated state observed in digestion studies [9]. Similarly, Koehl *et al*. observed a significant increase in the oral bioavailability of venetoclax using type-I based super LbF compared to lipid suspension in pigs [8]. In contrast, Siqueira *et al*. observed that type III super-LbF (50 mg/g formulation) exhibited comparatively lower cinnarizine exposure when compared to conventional LbF (20 mg/g formulation). These observations could be attributed to drug-specific factors, particularly the high propensity of cinnarizine to precipitate after the dispersion and digestion of super-LbF [20]. Recently, Paulus and colleagues investigated the influence of supersaturation on the absorption of cinnarizine from type I and type II LbFs. They observed a complex relationship between supersaturation and drug exposure, with supersaturation improving drug exposure more distinctly for type I LbFs compared to type II [21, 22]. Thus, there is a need to explore the correlation between *in vitro* findings and their influence on pharmacokinetic parameters, particularly for type III-based super-LbF formulations.

The current study aims to develop a super-LbF using a temperature-based supersaturation method across various drug loading levels for two model drugs, Ibrutinib (Ibr) and Enzalutamide (Enz). These drugs were chosen for their distinct physicochemical (log P and ionization behavior) and thermal characteristics (melting temperatures and T_m/T_g ratios) (Table I) [23–26]. The physical stability of super-LbF was comprehensively evaluated over an extended duration, using type III-A LbF as the prototype formulation. The prototype type III-A LbF was selected based on the higher drug solubility. Subsequently, the *in vitro* studies were conducted to assess the influence

Table I Physicochemical and Thermal Properties of Ibrutinib and Enzalutamide [25, 26]

Parameters	Ibrutinib	Enzalutamide
Molecular weight	440.5 g/mol	464.44 g/mol
Dissociation constant (pKa)	3.8 (weak basic)	Neutral
Log P	4.0	2.98
Polar surface area	99.2 $Å^2$	109 $Å^2$
Aqueous solubility in phosphate buffer (pH 6.5)	3 µg/mL	2.9 µg/mL
Melting peak Temperature (T_m)	158.11°C	200.83°C
Enthalpy of fusion (δhfus)	80.29 j/g	77.75 j/g
Crystallization peak temperature during cooling	N/A	N/A
Midpoint glass transition temperature (*T_g, midpoint)*	82.48°C	93.65°C
Crystallization peaks upon re-heating (*Tcryst, heat*)	N/A	N/A
T_m/T_g ratio	1.92	2.14
Approved maximum daily dose in human	560 mg (4 × 140 mg capsules)	160 mg (4 × 40 mg capsules)

of supersaturation on emulsification, and drug distribution in the aqueous phase. The results of these *in vitro* studies were then correlated to the absorption parameters obtained from pre-clinical pharmacokinetic studies in rats. This will help to understand the interplay between the physical attributes of the formulation and their resultant *in vivo* efficacy.

Materials & Methods

Materials

Ibrutinib (Ibr) as a gift sample was obtained from MSN Laboratories Pvt. Ltd. (Hyderabad, India). Enzalutamide (Enz) was obtained as a request sample from Zydus Lifesciences Ltd. (Ahmedabad, India). Abitec Corporation (Columbus, Ohio) provided Capmul® MCM EP (Glycerol Monocaprylocaprate) as a gift sample. Gattefossé (Co., France) provided Maisine® CC, Labrafac Lipophile® WL1349, Lauroglycol®, Peceol®, Labrasol® and Transcutol® HP. PEG 200 (Polyethylene glycol) was given by Thermo Fisher Scientific India Pvt. Ltd. (Mumbai, India). TRIS maleate salt, sodium hydrogen phosphate, sodium taurocholate hydrate, calcium chloride, and lecithin were provided by HiMedia Laboratories Pvt. Ltd. (Mumbai, India). Sigma-Aldrich (St. Louis, MO, USA) provided 4-bromophenylboronic acid, Kolliphor® RH40. Avra Synthesis Pvt. Ltd (Hyderabad, India) delivered Sodium hydroxide for the study. All experiments were conducted using purified water obtained from a Milli-Q purification system (Millipore, Bedford, MA). Other additional solvents and chemicals used in this study were of analytical grade.

HPLC Quantification Method

Chromatographic separation for Ibr and Enz was carried out using the Waters HPLC separation module and a GL Sciences reversed-phase C18 column (5 µm; 4.6 × 250 mm) at a temperature of 25 ℃. The chromatographic conditions for drug quantification of Ibr and Enz are provided in supporting information. Empower Pro software (Waters Corporation, California, USA) was used to acquire chromatographic data, which was extracted and analyzed at 260 nm and 237 nm wavelengths for Ibr and Enz, respectively. The analytical methods demonstrated a unidirectional, proportional relationship between concentration and the area under the curve for both drugs. The HPLC analytical method validation parameters are summarized in supporting information.

Solid-State Characterization of Model Drugs

Solid-state properties of Ibr and Enz were evaluated using polarized light microscopy, powder X-ray diffraction (PXRD), and differential scanning calorimetry (DSC). Polarized light microscopy was employed to identify the microscopic features of the powder drug samples. A Leica DMLP polarized microscope (Leica Microsystems Wetzlar GmbH, Germany) was used for this purpose, and the sample micrographs were captured using a Leica JVC digital camera and analyzed using Leica IM 50 software. The PXRD analysis was performed using an X-ray powder diffractometer (Rigaku, Japan). The applied voltage and current were 40 kV and 35 mA, respectively. The samples were mounted on stainless steel sample holders and were scanned in continuous mode between 3 – 40° (2θ), with a step size of 0.02°, and a scanning speed of 5 degrees/min. The same instrument conditions were used for precipitate analysis. Additionally, DSC (TA Q2000 DSC with

a refrigerated cooling accessory, TA Instruments, New Castle, DE) was employed to investigate the solid-state properties and T_m/T_g ratio for model drugs. The samples were prepared in hermetically sealed pans and were heated at 20°C/min to 10°C above the melting temperature, held isothermally for 3 min, cooled at a rate of 20°C/min to -20°C, and reheated at 20°C/min to just above the melting temperature in the heat-cool-heat mode. The sample weights for each repeat sample were within 2–3 mg.

Solubility Studies in Excipients and Lipid Solutions

In this study, solubility investigations were conducted at 37 ± 2°C using a variety of lipids, surfactants, and co-solvents, employing a previously reported method [27]. Different lipids and surfactants based on their chain length were used to prepare the different prototype formulations (composition details are represented in Table S1). Type II LbF is composed of 60% *w/v* lipids and 40% *w/v* surfactants, while type III formulation is prepared with 50% *w/v* lipids, 30% *w/v* surfactants, and 20% *w/v* co-solvent. The formulation is prepared by combining excipients in the aforementioned proportions, which are mixed and vortexed to form an isotropic clear solution [28]. In addition, a water shaker bath (Daihan Scientific, Korea) was used to determine drug solubility in various excipients and prototype lipid solutions, operated at 37 ± 2°C and 100 rpm for 48 h. The crystalline drug was added in excess to individual vials containing a measured amount of each excipient or lipid solution (1 g). After an equilibrium period, an adequate amount of samples was obtained, following the collection of supernatant after their centrifugation for 10 min at 10,000 rpm using iFuge UCo2R, (Neuation Technologies, Gujarat, India) [14]. Later, the collected supernatant was diluted with a 70:30% *v/v* mixture of ethyl acetate and methanol solution. Further, the resultant supernatant was diluted with methanol before being analyzed for drug content using HPLC conditions as described in the section 'HPLC quantification method'. The prototype lipid solution was chosen based on the maximum equilibrium solubility of drugs [29]. Furthermore, an evaluation of the impact of ambient and high temperature (25 ± 2°C and 60 ± 2°C) on drug solubility in the chosen prototype lipid formulations was performed [9, 30].

Preparation of Ibrutinib and Enzalutamide Lipid Formulations

The influence of supersaturation on liquid lipid formulation was evaluated by preparing LbF with three different drug loading. The detailed formulation compositions of lipid formulations for Ibr and Enz are provided in Table II.

Table II A detailed Description of Formulation Components of Conventional and Super-LbF

Ibrutinib formulations			
Formulation code	Conventional LbF	Super-LbF A	Super-LbF B
Capmul® MCM EP	500 mg	500 mg	500 mg
Labrasol®	300 mg	300 mg	300 mg
PEG 200	200 mg	200 mg	200 mg
Drug load (mg/g)	60 mg	120 mg	150 mg
aDS value	1	2	2.5
Enzalutamide formulations			
Formulation code	Conventional LbF	Super-LbF A	Super-LbF B
Capmul® MCM EP	500 mg	500 mg	500 mg
Labrasol®	300 mg	300 mg	300 mg
Transcutol®	200 mg	200 mg	200 mg
Drug load (mg/g)	32 mg	64 mg	80 mg
aDS value	1	2	2.5

Conventional LbF

Conventional LbF was formulated using 50% *w/v* of oil, 30% *w/v* of surfactant, and 20% *w/v* of co-solvent. The drug payload of each model drug was maintained at 100% of its equilibrium solubility (measured at 25 ± 2°C) in the lipid solution. Following drug loading, the formulations were vortexed to achieve a clear solution.

Super-LbF

Super-LbF was formulated with high drug loading wherein drug concentration exceeded than its equilibrium solubility in the lipid solution. Higher drug loading was attained through a temperature-based supersaturation method. In this process, the lipid solution was heated to 60 ± 2°C, facilitating drug supersaturation, followed by cooling to room temperature [10]. The procedure was repeated to obtain a clear solution. In this study, two different super-LbF were prepared with varying drug loadings based on their equilibrium solubility in the lipid solution (Table II).

Physical Stability Evaluation

The physical stability of prepared formulations was monitored for 60 days of storage at 25 ± 2°C and 65 ± 5%RH. The samples were stored in closed glass vials throughout the stability analysis. Visual assessments and polarized light microscopy were performed at pre-defined time points. Samples were withdrawn from different locations within the glass vial, placed on a curved glass slide, and observed under the polarized light microscope (Leica, Germany).

Drug content was determined at each time interval to assess the chemical stability. Every collected sample was centrifuged for 10 min at 10,000 rpm, to allow solid particles

to settle down. Subsequently, 50 mg of the supernatant was diluted with a 70:30% *v/v* mixture of ethyl acetate and methanol solution. Further dilution of resultant supernatant with methanol before being analyzed for content of drug using HPLC conditions as described in the section 'HPLC quantification method'.

In Vitro Dispersion Studies

The prepared LbF were studied for droplet size, polydispersity index (PDI), and zeta potential using the Zetasizer Nano ZS instrument (Malvern Instruments, Worcestershire, UK). For this analysis, 100 mg of each liquid formulation was diluted with milli-Q water up to 20 mL in a glass vial. An emulsion was created by gently reversing the vial multiple times. Subsequently, a 1 mL aliquot was extracted and analyzed in triplicate using a disposable ZEN0040 cuvette for droplet size and a DTS1070 cuvette for zeta potential.

In Vitro Digestion Study

The high throughput lipolysis method reported by Kilic and Dressman was used to assess the impact of aDS on the aqueous drug solubilization in digestive conditions [31]. Briefly, each formulation was dispersed in a digestion buffer (36 mL) to simulate human fasted-state intestinal conditions. The composition details of the media are provided in Table S2. The initial experimental period (0–10 min) focused on the dispersion behavior of the formulation, which was obtained by stirring it in the digestion medium. Aliquots (~ 0.5 mL) were removed from the media at predefined time points of 2.5, 5, and 10 min relative to the start of dispersion. The samples were centrifuged at 37°C and 15,000 rpm for 10 min and analyzed for aqueous phase and pellet phase drug concentration. After completion of the dispersion phase, the digestion process was initiated by adding 4 mL of pancreatic extract to the solution. The addition of 0.6 M NaOH solution to the media maintained a 6.5 pH throughout the experiment. Aliquots (~ 0.5 mL) from the digestive media were collected at predefined time points of 5, 15, 30, 45, and 60 min relative to the initiation of digestion. Further digestion was prevented by the prior addition of lipase inhibitor (4-bromophenylboronic acid, 5 µL/mL of 1 M in methanol) to every micro-centrifuge sample tube. The samples were then instantly centrifuged for 10 min at 15,000 rpm and 37°C using a laboratory centrifuge to collect an aqueous solubilized phase. The aqueous phase was analyzed for its drug concentration using the protocol mentioned in the section 'HPLC quantification method'. After phase separation by centrifuging the digestion media, the resultant pellet was carefully extracted from polypropylene tubes. These pellets were then transferred onto a glass plate and air-dried at ambient temperature. Then the dried samples were monitored for their solid-state characteristics using powder X-ray diffraction [18]. The precipitate characterization was performed for super-LbF B (as a representative super-LbF) to assess the physical form of the precipitate compared with the unformulated crystalline drug. The instrumental conditions for PXRD analysis are provided in the section 'Solid-state characterization of model drugs.

In Vivo Pharmacokinetic Study

Ethics Approval

The animal study protocol received approval from the institutional Animal Ethics Committee of the National Institute of Pharmaceutical Education and Research (NIPER), S.A.S. Nagar, and is duly registered with the Committee for the Purpose of Control and Supervision of Experiments on Animals (CPCSEA) under registration number 108/1999/CPCSEA. The approval numbers for the study protocols related to Ibr and Enz are IAEC/22/47 and IAEC/23/72, respectively. For pharmacokinetic studies, the animals involved in this study were accommodated in the Central Animal Facility at NIPER, S.A.S. Nagar. They were housed in plastic cages, adhering to standard laboratory conditions, which include maintaining a natural 12-h light–dark cycle. The animals had *ad libitum* access to a conventional rodent dry diet and water. Each study group consists five number of animals.

Ibrutinib

In the pharmacokinetic evaluation of Ibr formulations, female Sprague Dawley rats (weighing 180–220 g) received oral administrations of crystalline drug suspension, conventional LbF, and super-LbF. super-LbF with the highest Ibr loading was selected for further pharmacokinetic evaluation to assess the impact of supersaturation and formulation quantity. Sodium carboxymethyl cellulose (0.2% *w/v*) was used as a suspending agent to disperse the crystalline drug in purified water. Each group of five animals received a 20 mg/kg dose of Ibr in a 10 mL/kg volume [32]. Following oral administration, blood samples of approximately 0.2 mL were obtained from the tail vein at predetermined intervals (0.5, 1, 1.5, 2, 4, and 8 h). Subsequently, the collected samples underwent centrifugation at 5000 rpm for 5 min to separate the plasma.

Enzalutamide

The pharmacokinetic assessment of Enz formulations was conducted in male Sprague Dawley rats weighing between 200–220 g. The study involved the oral administration of crystalline drug suspension, conventional LbF, and super-LbF. Super-LbF with the highest Enz loading was used for

further pharmacokinetic evaluation to assess the impact of supersaturation. Each group of five animals received a 30 mg/kg dose of Enz in a 10 mL/kg volume [24]. After administration, blood samples (approximately 0.2 mL) were collected at specified intervals (0.5, 1, 2, 4, 8, 12, 24, 48, and 72 h), followed by centrifugation at 5000 rpm for 5 min to separate the plasma.

Plasma Sample Analysis

For quantitative analysis, plasma samples underwent processing using the liquid–liquid extraction method. Specifically, 10 µL of the internal standard and 200 µL of acetonitrile: methanol (in a 50:50 ratio, used as a precipitating agent) were added to 100 µL of the collected plasma samples. Sorafenib and diclofenac were used as internal standards for the quantitative determination of Ibr and Enz, respectively. The mixture was vortexed for a few minutes and then centrifuged for 10 min at 10,000 rpm using iFuge UCo2R, (Neuation Technologies, Gujarat, India). The resulting supernatant was collected into a microcentrifuge tube, followed by evaporation of the supernatant using a vacuum concentrator. The final dried residue was re-dispersed with 160 µL of acetonitrile: water (9:1) and subjected to drug quantification using HPLC. The detailed bioanalytical method specifications and validation results are given in supporting information.

Statistical Analysis

All the experiments were performed in triplicate, and the results are presented as mean ± standard deviation. The student's t-test and ANOVA were employed to identify statistically significant differences between two groups and more than two groups, respectively, using GraphPad Prism® (version 8.4.2), with a significance level set at p-value < 0.05. The pharmacokinetic parameters based on the non-compartmental analysis were calculated by using the PK-Solver, a freely available menu-driven add-in program for Microsoft Excel.

Result and Discussion

Solid State Characterization of Model Drugs

The identification of the crystalline form of Ibr was carried out using different analytical tools, and irregularly shaped crystals were observed in the optical mode of the microscope. In the polarized mode, birefringence was observed due to the anisotropic crystalline nature of the Ibr (Figure S1A). The Enz was found to be a white, non-hygroscopic crystalline powder with an irregular shape of crystalline structure observed in the polarized mode microscope (Figure S1B). The PXRD spectrum of Ibr and Enz (Figure S2) exhibited several intense and sharp peaks, confirming its crystalline nature. In this study, we also conducted thermal characterization of model drugs through DSC heating–cooling-heating experiments. Figure S3 depicts the resulting DSC thermograms, and the characteristic temperatures, enthalpies from observed thermal events, and the T_m/T_g ratio for each compound are summarized in Table I. The DSC heating curves (first heating cycle) revealed distinct endothermic peaks for Ibr and Enz, occurring at 156–158°C and 198–201°C respectively [23, 26]. During the cooling and reheating cycles, no endothermic event was observed for either of the drugs. Further, Enz exhibited a higher T_m/T_g ratio of 2.14 compared to Ibr, which had a ratio of 1.92. Fridgeirsdottir *et al*. suggest that a higher T_m/T_g ratio is linked to an elevated propensity for drug crystallization [33]. This finding suggests that Enz may have a greater tendency to crystallize than Ibr, which could have implications for drug loading and the physical stability of the formulation.

Solubility Study in Excipients and Lipid Solutions

Solubility investigations were carried out at 37 ± 2°C using a range of lipids, surfactants, and co-solvents utilizing a previously reported method [27]. A variety of lipid excipients were used, based on chain length long chain length (LC), and medium chain (MC). Amongst the MC-based lipids, investigated, Capmul® MCM EP demonstrated the highest solubility value. Specifically, it exhibited a significant solubility of 44.07 ± 4.7 mg/g for Ibr and 12.91 ± 2.0 mg/g for Enz (Fig. 1a and c). In contrast, lipid vehicles based on long-chain triglycerides (LC) exhibited the lowest solubility for both drugs. The tendency of higher drug solubility in MC-based lipids than LC-based lipids can be ascribed to drug-specific interactions with the length of the lipid chains and the nature of the lipid vehicle [29]. Evaluation of surfactants revealed promising solubility outcomes for both drugs. Ibr exhibited solubility values of 35.72 ± 1.68 mg/g in Labrasol® and 31.06 ± 3.84 mg/g in Kolliphor® RH 40, while Enz demonstrated maximum solubility in Labrasol® (57.7 ± 5.6 mg/g) and Tween® 20 (24.4 ± 3.5 mg/g) (Fig. 1b and e). Furthermore, PEG 200 and Transcutol® were identified as optimum solubilizers based on their maximum solubilization capacity for Ibr and Enz, respectively, as depicted in Fig. 1c and f. The results indicate that the compound's thermal behavior significantly influences its solubility value. Using the selected excipients, prototype lipid formulations were prepared through the admixture method and the detailed compositions of these prototype formulations are presented in Table I. The prototype formulations were selected based on criteria such as miscibility and solubility for both drugs (Table S1, supporting information).

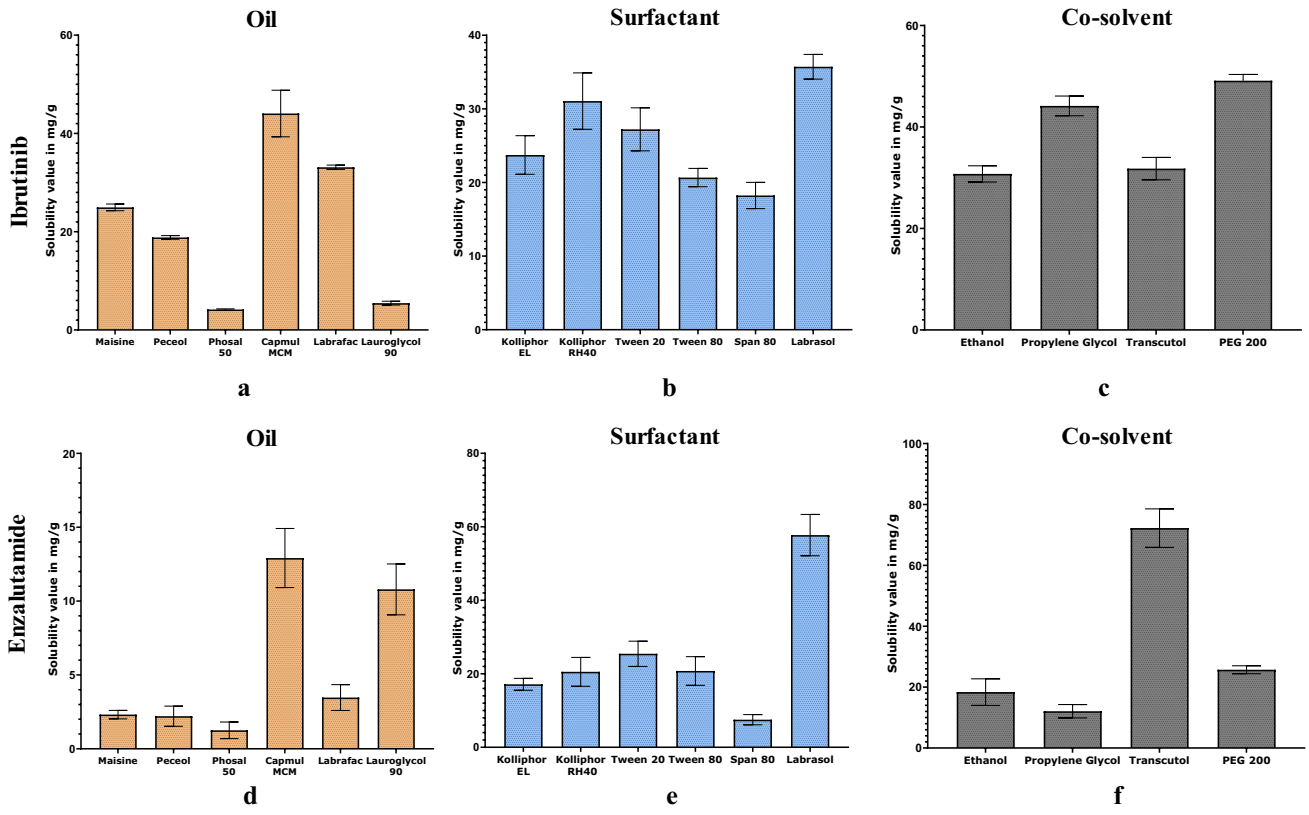

Fig. 1 Equilibrium solubility of ibrutinib **a**, **b** & **c** and enzalutamide **d**, **e** & **f** in oil components, surfactants, and co-solvents at 37 ± 2°C

Table III Temperature-Dependent Solubility and aDS Values for Ibrutinib and Enzalutamide at 25 ± 2°C, 37 ± 2°C, and 60 ± 2°C

Parameters	Ibrutinib	Enzalutamide
Solubility at 25 ± 2°C (mg/g)	60.15 ± 6.74	31.09 ± 0.55
Solubility at 37 ± 2°C (mg/g)	73.68 ± 1.81	44.62 ± 6.14
Solubility at 60 ± 2°C (mg/g)	161.03 ± 9.19	75.15 ± 4.59
aDS at 37 ± 2°C	1.22 ± 0.12	1.43 ± 0.18
aDS at 60 ± 2°C	2.68 ± 0.14	2.41 ± 0.15

Influence of Temperature-Induced Supersaturation on the Drug Loading in LbFs

The study assessed the impact of temperature on the drug solubility in the chosen prototype formulation, which is a type IIIA formulation (compositions are represented in Table II) [34]. The study results (Table III), indicate that drug solubility increased significantly when examined at elevated temperatures compared to room temperature. Particularly noteworthy was the 2.5 to 2.7-fold increase in Ibr concentration observed when heated at 60 ± 2°C (161.03 ± 9.19 mg/g), in comparison to 25°C (60.15 ± 6.74 mg/g). A similar trend was observed for Enz, where solubility increased to 75.15 ± 4.59 mg/g at 60 ± 2°C compared to 31.09 ± 0.55 mg/g at 25 ± 2°C. The observed trend highlights the importance of temperature-induced drug supersaturation within lipid vehicles by overcoming crystal lattice energy. Specifically, lower crystallization lattice energies (in the case of Ibr) were found to promote greater drug dissolution in lipid vehicles due to weaker intermolecular forces within the crystal lattice [35].

Furthermore, determining the degree of supersaturation in a lipid solution is crucial for establishing the drug loading. aDS values were determined and the results are shown in Table III. The chosen formulation demonstrated minimal enhancement in the aDS at 37°C for both drugs. In contrast, higher aDS values of 2.68 ± 0.14 and 2.41 ± 0.15 were achieved for Ibr and Enz, respectively, when the formulation was prepared at a temperature of 60 ± 2°C. A similar trend was noted with celecoxib and cinnarizine, where aDS values ranging from 1.5 to 2.5 were achieved using the thermal-induced supersaturation method [19]. Additionally, Bennett-Lenane *et al*. conducted a retrospective analysis of data from 21 distinct super-LbFs. Their findings concluded that both MC-based and LC-based LbFs exhibited a similar degree of supersaturation (1–3.5) when heated at 60 ± 2°C [15]. Based on the assessed aDS value, three distinct drug loading levels were identified for further examination. The detailed formulation compositions are given in Table II. The drug loading

for conventional LbF was equal to equilibrium solubility in the lipid solution while super-LbF A and super-LbF B featured drug loads surpassing the equilibrium solubility of drugs.

Influence of Degree of Supersaturation on the Physical Stability of LbF

In this study, the conventional and super-LbFs were kept at room temperature stability conditions (25°C/65% RH) for 60 days. The microscopic evolution was carried out under a light microscope to check the generated drug particle within the formulation and results are represented in Fig. 2. The conventional formulation and super-LbF A of Ibr exhibited no discernible signs of drug crystallization throughout the 60-day observation period. However, contrasting results were observed in the microscopic images of super-LbF B, revealing the presence of drug crystals within the formulations at a 60-day time point. These findings align with previously reported outcomes by Ilie *et al*. in 2020, where lipid formulations with a lower degree of supersaturation within the range of 1–2 aDS values showed a low risk of precipitation on short-term storage, and crystallization tendency increased for higher degrees of supersaturation (> 2 aDS values) [19]. Additionally, the drug content analysis revealed a reduction in the original content after the 60-day time interval (p-value > 0.05), as depicted in Fig. 3a.

In the case of Enz formulations, conventional LbF remained stable throughout the study period whereas both super-LbFs exhibited drug crystallization after 60 days of storage. The microscopic evaluation revealed the generation of non-uniformly shaped crystals for the Enz containing super-LbFs, as illustrated in Fig. 2. These observations suggest that drug crystallization within the liquid preconcentrate is dependent upon the inherent characteristics of the drug and the achieved aDS in the lipid solution [15, 19]. The tendency of Enz to undergo re-crystallization in the liquid LbF has been previously documented [36]. The drastic reduction in drug content over the storage period is also evident in Fig. 3b (p-value < 0.05). Similarly, Bannow *et al*. demonstrated that the increased thermodynamic driving force is responsible for drug re-crystallization within lipid solution due to the higher degree of supersaturation (aDS value of 2.5) and the onset of precipitation time was within 24 h [18]. Furthermore, the differences in the physicochemical properties of Enz and Ibr, such as lipophilicity and melting point, also affect their physical stability. Overall, these findings suggest that an enhanced degree of supersaturation within the formulation may pose the risk of drug precipitation over a longer period of storage.

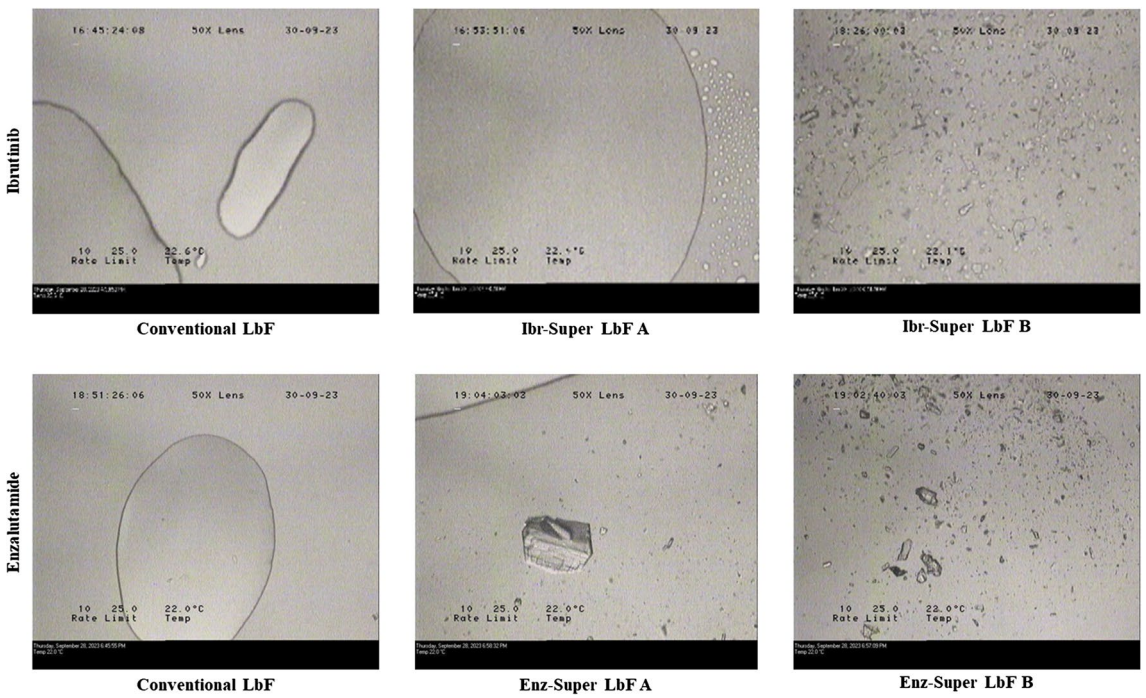

Fig. 2 Evaluation of the physical stability of conventional LbF and super-LbF through microscopic evaluation. The microscopic images are captured at 50 × magnification power for 60-day samples

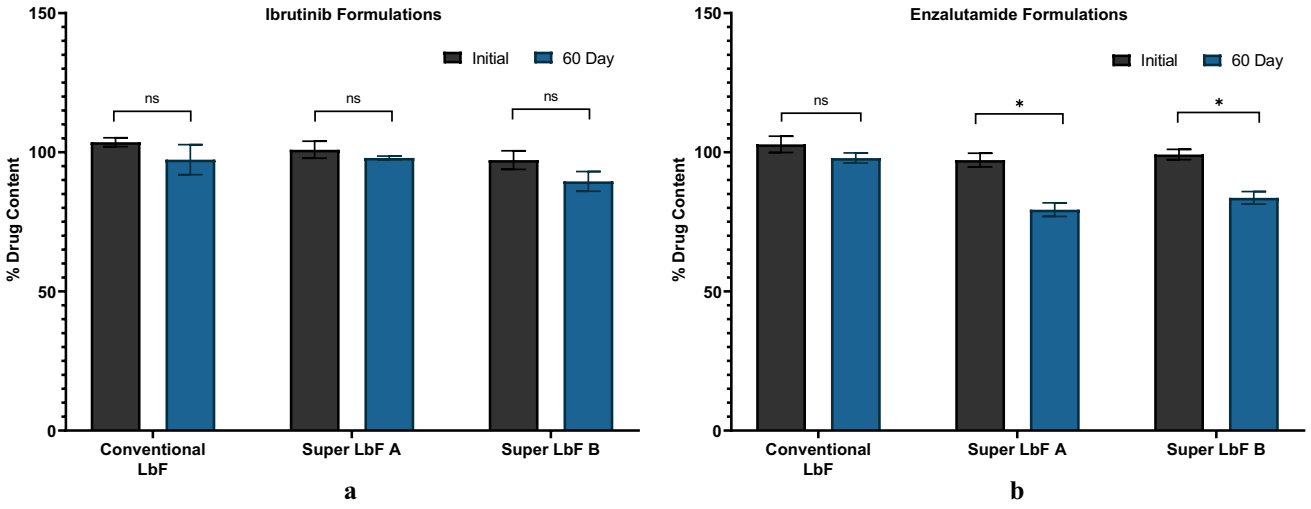

Fig. 3 Drug content determination for ibrutinib **a** and enzalutamide **b** formulations after 60 days of storage. A paired student t-test analysis was conducted to assess statistical significance. The results showed that '*' represents a statistically significant difference (p-value < 0.05), and "ns" denotes a non-significant difference with initial values

Influence of Degree of Supersaturation on Dispersion Behavior of LbF

To examine the effect of the degree of supersaturation on dispersion behavior, the average droplet size, PDI value, and zeta potential were evaluated for both initial and after a 2-h period of aqueous dispersion. In the case of Ibr, conventional LbF exhibited a mean droplet size of 245 ± 20 nm with 0.350 ± 0.02 as a PDI value at the initial time of dispersion (Fig. 4a and b). No substantial differences in these values were detected after 2-h of dispersion, indicating the stability of the emulsion.

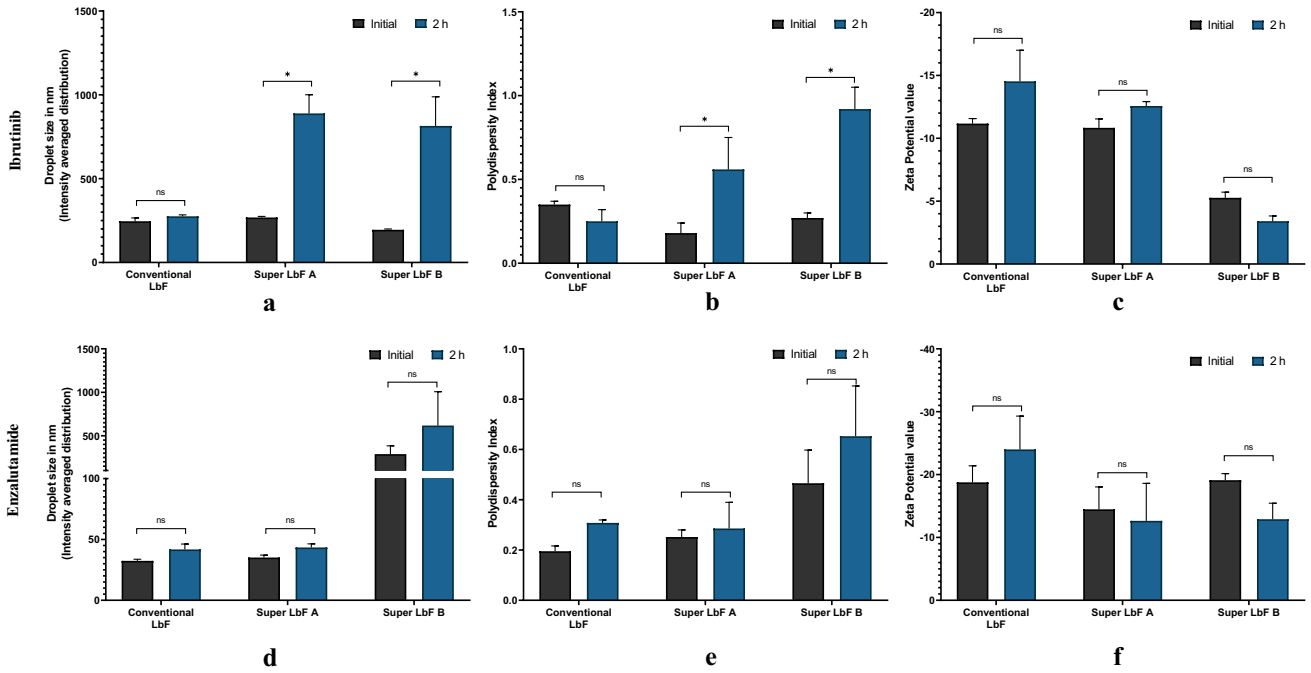

Fig. 4 Dispersion behavior i.e. average droplet size **a** & **d**, polydispersity index value **b** & **e**, and zeta potential **c** & **f** of conventional LbF and super-LbFs for ibrutinib and enzalutamide. The sample measurements ($n = 3$) were performed both initially and after a 2-h period of aqueous dispersion. The results showed that '*' represents a statistically significant difference (p-value < 0.05), and "ns" denotes a non-significant difference with initial values

The zeta potential values for the conventional lipid-based formulation at the initial time of dispersion and after 2-h were -11.17 ± 0.40 and -14.53 ± 2.48, respectively (Fig. 4c). However, the increase in the aDS within the LbFs resulted in significant changes in dispersion parameters after a 2-h dispersion period (p value < 0.05) which might be due to dilution-mediated drug precipitation [37]. As illustrated in Fig. 4, a drastic increase in droplet size and PDI values was observed for super-LbF after 2-h of dispersion.

For Enz, both conventional and super-LbF A maintained consistently low droplet sizes and PDI values, even after a 2-h aqueous dispersion. However, in contrast, super-LbF B (with an aDS value of 2.5) exhibited an increase in the droplet sizes and PDI values after 2-h of dispersion, as evidenced by Fig. 4d and e. The zeta potential shifted from -19.10 ± 1.04 initially to -12.90 ± 2.54 after 2-h (Fig. 4f). This shift is likely due to changes in particle interactions or aggregation within the dispersion [38]. In comparing both drug formulations, it appears that the amount of drug load significantly influences the overall droplet size and dispersion parameters. This phenomenon may be due to a substantial quantity of drug dissolved in liquid preconcentrate and a decrease in solubilization capacity upon dilution. The difference in zeta potential observations of super-LbF also signifies the physical instability of emulsion [38].

Influence of Degree of Supersaturation on Aqueous Phase Drug Distribution of LbF

The aqueous solubilization of drugs is a crucial factor that influences the *in vivo* oral bioavailability of LbFs. Moreover, the characteristics of solubilizing species and drug precipitates formed during lipolysis serve as pivotal determinants governing *in vivo* performance. In this study, we assessed the influence of drug loading in LbF on drug solubilization through an *in vitro* high throughput lipolysis experiment, as reported by Kilic and Dressman [31].

Ibrutinib Solubilization in Digestive Conditions

Figure 5a depicts a decreasing pattern in the solubilization profiles of both conventional and super-LbFs under digestive environments. In the dispersion phase, all Ibr formulations exhibited a subtle decline in drug concentration, whereas a rapid decrease was observed after the initiation of the digestion process, regardless of the drug loading levels. The rapid decline in drug concentration could be attributed to the diminished solubilization capacity on digestion, particularly notable for the type III formulation [39]. By completion of the study, the drug concentration moves toward its equilibrium solubility in the digestion media, reaching approximately 26 µg/mL. It was also noted that a low amount of lipid solution (for super-LbFs) did not show a significant impact on the aqueous drug solubilization in the digestive condition (p-value > 0.05).

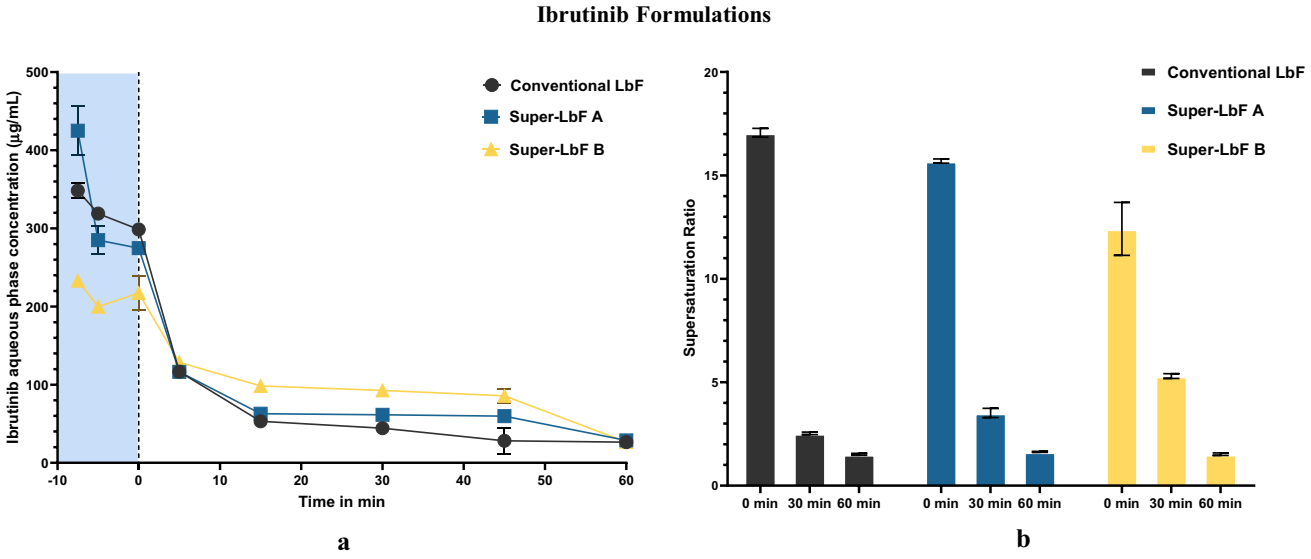

Fig. 5 **a** Aqueous drug phase distribution of conventional LbF and super-LbFs in the digestive condition for ibrutinib. The blue region indicates the dispersion phase and the remaining profile represents the digestion phase. The vertical dotted line on the x-axis at 0 min indicates the initiation of the digestion phase. **b** The supersaturation ratio (SR) value for ibrutinib was obtained at 0 min, 30 min, and 60 min of the lipolysis process

The apparent equilibrium solubility of Ibr in post-digestive media was found to be 17.5 ± 2.6 µg/mL. The supersaturation ratio was determined by calculating the amount of solubilized drug concentration to the apparent equilibrium solubility of Ibr in post-digestive media at different time points. During the dispersion stage, a higher supersaturation ratio (SR value ~ 11–15) was achieved for all the formulations. Devraj *et al*. previously reported similar observations, demonstrating that MC-based formulations induce the formation of a supersaturated concentration of the drug in the dispersion phase [40]. However, during the digestion process, the solubilization capacity in the colloidal phase decreased, resulting in lower SR values observed at 30 min as well as 60 min post-lipolysis, as represented in Fig. 5b. There are two plausible mechanisms for the reduction in the solubilization capacity of conventional LbF and super-LbF. First, during digestion, the hydrolysis of triglycerides releases free fatty acids into the gastrointestinal milieu. These free fatty acids have a propensity to associate with drug molecules, enhancing their solubilization due to their amphiphilic nature and ability to form micelles. However, despite the initial enhancement in solubilization, the endogenous absorption of free fatty acids can subsequently lead to a reduction in micellar solubilization capacity. This occurs as a result of the increased presence of ionized free fatty acids in the intestinal environment. The microclimate pH gradient between the unstirred water layer and the intestinal lumen promotes the protonation of free fatty acids, converting them into their ionized forms. The ionized form of free fatty acids exhibits greater solubility in aqueous environments compared to their non-ionized counterparts, thereby reducing their availability to solubilize drug molecules within micelles [41, 42]. Second, the presence of surfactants and co-solvents in a liquid preconcentrate can reduce the concentration of the solubilized drug. This reduction occurs because the hydrophilic components are miscible with the aqueous medium, leading to a loss in apparent solubility. Consequently, this results in transient supersaturation within the colloidal phase [4, 29, 43, 44].

Enzalutamide Solubilization in Digestive Conditions

The concentration profile of Enz in the aqueous phase under digestive conditions, as influenced by different levels of drug payload, is summarized in Fig. 6a. During the dispersion phase, the concentration of Enz remained solubilized (at 83.23 ± 14.38 µg/mL) for the conventional LbF formulation. Conversely, in the case of super-LbFs, the solubilized Enz level experienced a rapid decline during the dispersion phase. The calculated SR value for each formulation at different intervals of dispersion and digestion phase is summarized in Fig. 6b. Under the conditions of digestion, the conventional LbF formulation displayed a gradual decrease, reaching a concentration of 18.52 ± 3.32 µg/mL at the end of the experiment. Both super-LbF formulations exhibited comparable profiles despite differences in drug payload and lipid amounts, with the concentration levels approaching near-equilibrium solubility concentration. The measured equilibrium solubility of Enz was determined to be 4.45 ± 0.98 µg/mL in the post-digestive medium.

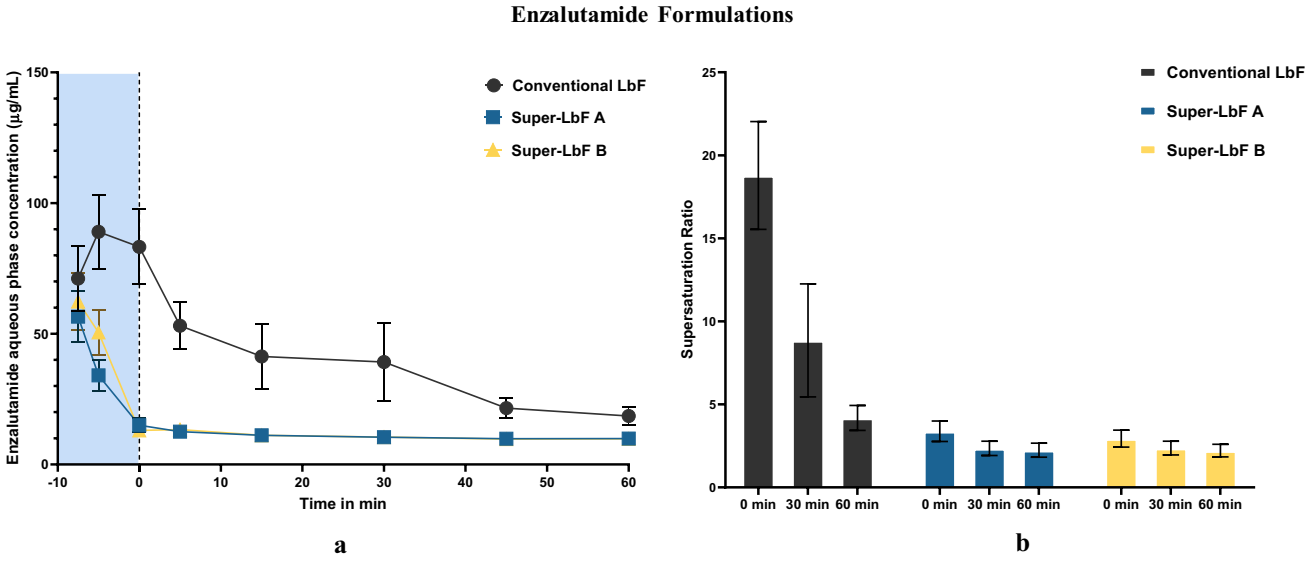

Fig. 6 **a** Aqueous drug phase distribution of conventional LbF and super-LbFs in the digestive condition for enzalutamide. The blue region indicates the dispersion phase and the remaining profile represents the digestion phase. The vertical dotted line on the x-axis at 0 min indicates the initiation of the digestion phase. **b** The supersaturation ratio (SR) value for enzalutamide was obtained at 0 min, 30 min, and 60 min of the lipolysis process

In this study, it was observed that the lipophilicity of the drug, and the quantity of formulation substantially influence the distribution of the drug in the aqueous phase. The amount of formulation used during the digestion study also governs solubilization by altering the colloidal structures. In the case of the super-LbFs, the low quantity of lipids may be accountable for the generation of a lower portion of the digestive product or colloidal species, resulting in lower solubility in the digestive phase. Conversely, a high portion of lipid mass results in the generation of a lipid-rich phase, which improves the association with lipophilic drugs and enhances the apparent solubilization [45]. Overall, the amount and type of formulation, drug payload, and inherent characteristics (lipophilicity) of the drug are accountable for the reduction in solubilization capacity, thereby leading to the generation of transient supersaturation for both drugs [43]. The transient supersaturated state is highly thermodynamically unstable, leading to the precipitation of the drug. Hence, solid-state analysis was performed on the precipitate obtained after digestion to identify its nature.

Precipitate Characterization

The physical characteristics of drug precipitates play a vital role in influencing drug absorption in the intestinal region [44]. The diffraction patterns of the blank digest, crystalline Ibr, and obtained precipitate are shown in Fig. 7a. The crystalline Ibr showed characteristic diffraction peaks at 2θ values of 5.60, 10.57, 12.24, 13.51, 16.01, 16.55, 18.21, 19.72, 21.16, 21.56, 23.39, 26.40 and 28.77 [32]. The obtained precipitate after the lipolysis study of Super-LbF (high drug loading level) also showed characteristic peaks of crystalline Ibr with slight deviations. Similarly, the assessment was conducted for Enz super-LbF following the digestion experiment and the PXRD overlay is presented in Fig. 7b. The PXRD overlay confirms the crystalline nature of the precipitated drug, as evidenced by the presence of characteristic peaks resembling those of crystalline Enz. In this study, the effect of the physicochemical properties (ionization and melting point) of these drugs had a similar impact on the nature of the physical form of the precipitate. The crystalline nature of the precipitate could be detrimental to drug absorption as it may reintroduce the dissolution step. However, these observations lack confirmatory validity, as the physical form of the precipitate may undergo alterations with increased sample processing time, indicating a limitation of the current study. In the future, advanced real-time analytical approaches can be used to identify the true nature of the precipitate without interfering with the sample [5, 46].

Pharmacokinetic Study

To validate the *in vitro* findings, an *in vivo* pharmacokinetic study was performed using Sprague Dawley rats after every oral administration of the prepared formulation. In this study, conventional LbF and super-LbF (highest drug payload) were employed to investigate the influence of drug loading levels and enhanced drug solubilization under *in vivo* conditions. Crystalline aqueous suspensions were used as a control group for each drug.

In Vivo Fate of Ibrutinib After Oral Administration

Figure 8a illustrates the plasma concentration–time profiles after the oral administration of crystalline Ibr suspension, conventional LbF, and Super-LbF B. A Summary of calculated pharmacokinetic parameters is represented in Table IV. Crystalline Ibr demonstrated constrained pharmacokinetic

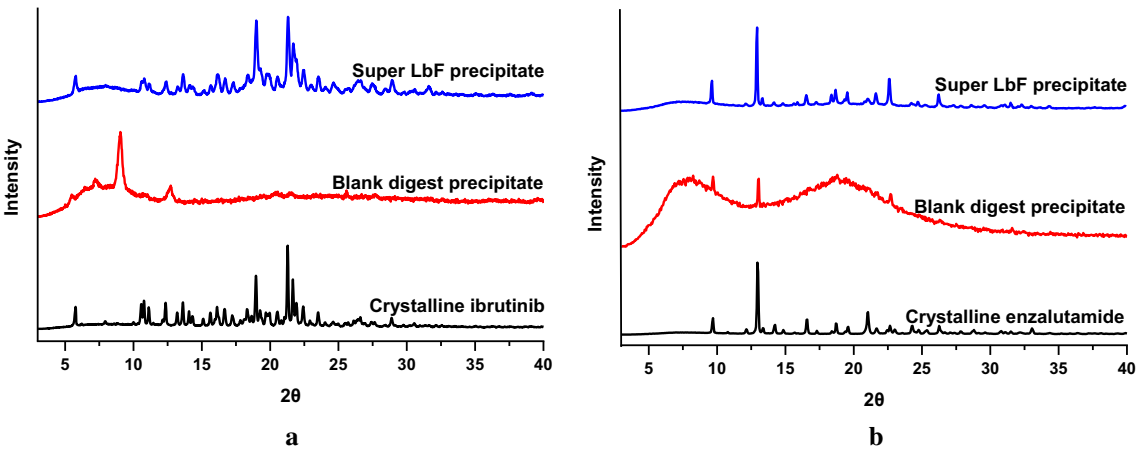

Fig. 7 PXRD overlays of the precipitate obtained after the lipolysis of super-LbF (highest drug payload) of ibrutinib **a** and enzalutamide **b**. The diffraction patterns of the blank digest, crystalline drug, and the obtained precipitate after lipolysis of the super-LbF (highest drug payload) were compared

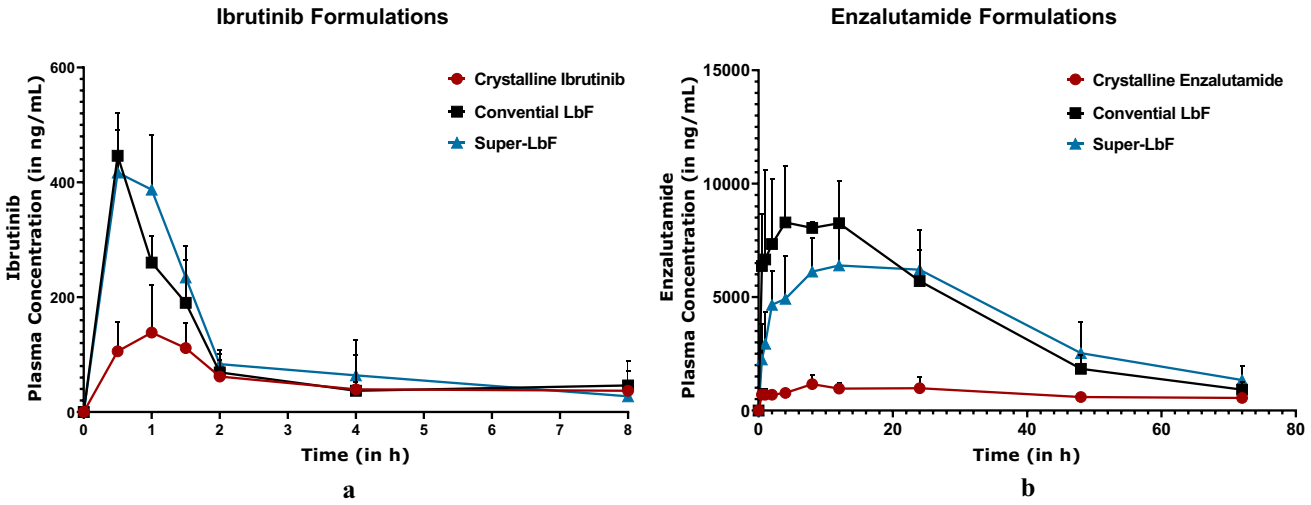

Fig. 8 **a** Plasma concentration–time profiles after the oral administration of crystalline ibrutinib suspension, conventional LbF, and super-LbF (highest drug load) at a dose of 20 mg/kg in Sprague Dawley rats. **b** Plasma concentration–time profiles after the oral administration (30 mg/kg equivalent dose) of crystalline enzalutamide suspension, conventional LbF, and super-LbF (highest drug load)

Table IV Pharmacokinetic Parameters After Oral Administration of Ibrutinib and Enzalutamide Formulations

Model drugs (administered dose)	Orally administered formulations	Pharmacokinetic Parameters	
		C_{max} (ng/mL)	AUC (ng*h/mL)
Ibrutinib (20 mg/kg)	Crystalline Ibr	147.49 ± 73.53	461.33 ± 168.83
	Conventional LbF	398.27 ± 180.25*	666.39 ± 289.58#
	Super-LbF B	458.42 ± 80.48*	797.28 ± 137.70*
Enzalutamide (30 mg/kg)	Crystalline Enz	1372.79 ± 784.02	55,217.22 ± 33,917.81
	Conventional LbF	9858.09 ± 2001.96*	300,176.52 ± 42,196.45*
	Super-LbF B	7424.31 ± 897.28*	289,262.92 ± 65,008.87*

All the data are represented as mean ± standard deviation (no. of animal used for each group = 5)

"*" represents a significant difference when compared to respective crystalline drug suspension

"#" represents no significant difference was observed compared respective crystalline drug suspension

parameters, with a C_{max} of 147.49 ± 73.53 ng/mL and an AUC value of 461.33 ± 168.83 ng*h/mL. Both lipid formulations demonstrated higher drug exposure, as evidenced by elevated C_{max} and AUC values when compared to the crystalline suspension. The plasma concentration profile suggests that the initial phase of the pharmacokinetic profile, especially within the first 2-h time, is sensitive to formulation changes, which impacts absorption. This sensitivity includes factors such as drug supersaturation and the maintenance of a metastable state, impacting early drug absorption and disposition. Among the lipid formulations, both the conventional LbF and Super-LbF B demonstrated comparable maximum concentration (C_{max}) values, with specific values of 398.27 ± 180.25 ng/mL and 458.42 ± 80.48 ng/mL, respectively (p value > 0.05). AUC values were found to be 666.39 ± 289.58 ng*h/mL and 797.28 ± 137.7 ng*h/mL for conventional LbF and Super-LbF B, respectively (p value > 0.05). No major variation in pharmacokinetic parameters was identified between conventional and Super-LbFs in *in vivo* settings (p-value > 0.05). The upsurge in pharmacokinetic parameters within 2-h for both formulations may be attributed to the initial phase of drug supersaturation in the digestive conditions. Similar observations regarding intestinal absorption were also noted in the case of fenofibrate-based type IIIA MC-based LbF, wherein the formulations demonstrated the capability to induce transient supersaturation for a shorter duration (up to 1-h). However, in the later absorption phase, a marked difference was observed due to drug precipitation [41]. In contrast, Siqueira *et al*. observed that type III Super-LbF (50 mg/g formulation) exhibited comparatively lower cinnarizine exposure when compared to conventional LbF (20 mg/g formulation). These observations could be attributed to the high propensity of cinnarizine to precipitate after the dispersion and digestion of Super-LbF. The reason for the aforementioned finding could be drug-specific absorption and the imbalance

of the supersaturated state in the intestinal region [20]. Overall, the short time duration of the thermodynamic metastable state during the digestive condition may impede the potential benefits of supersaturating formulations. The quantity of lipid formulation used for the pharmacokinetic study did not significantly influence the drug exposure, as the low quantity used in the Super-LbF B formulation resulted in similar drug exposure levels to those observed with the conventional LbF, despite the larger amounts administered in the conventional LbF [47].

In Vivo Fate of Enzalutamide After Oral Administration

Similarly, pharmacokinetic studies in Sprague–Dawley rats were conducted for the Enz formulations, and the plasma concentration–time profile is depicted in Fig. 8B. Statistical analysis by one-way ANOVA suggests significantly higher exposure after administration of both the conventional LbF and super-LbF of Enz compared to the free Enz suspension. (p-value < 0.05), as detailed pharmacokinetic parameters are provided in Table IV. However, the limited absorption observed with crystalline Enz is constrained by dissolution limitations and these results align well with previous reports [218]. Among the lipid formulations, Conventional LbF exhibited a comparable rate and extent of absorption (in terms of Cmax and AUC values) to Super-LbF with a non-significant difference (p-value > 0.05). The conventional LbF has a C_{max} and AUC value of 9.8 ± 2.0 µg/mL and 300.17 ± 42.19 µg*h/mL, respectively. While the C_{max} and AUC values for the Super-LbF B were 7.4 ± 0.8 µg/mL and 289.26 ± 65.00 µg*h/mL respectively. However, the observed variations in Enz solubilization behavior between conventional LbF and Super-LbF are not significantly reflected in the pharmacokinetic outcomes associated with these formulations. The observed differences could be attributed to the variations between the *in vitro* setup and the *in vivo* gastrointestinal conditions in rats, including factors such as gastric emptying and luminal content, which were not considered in this study. Additionally, the non-sink conditions employed in the *in vitro* setup may not accurately predict the *in vivo* luminal behavior [9, 48].

Overall, the pharmacokinetic results of Super-LbF showed comparable results with a low volume of formulation (due to high drug load) in comparison to conventional LbF (which required a higher formulation quantity due to low drug load). These observations indicate that Super-LbF can deliver the desired dose with a low volume of formulation excipient, potentially reducing formulation costs. Super-LbF has successfully addressed the challenge associated with limited drug loading and higher pill burden providing comparable benefits with conventional LbF in preclinical studies. Moreover, the observed pharmacokinetic results for both drugs are well corroborated with Thomas *et al.* and Siqueira *et al.* [48, 49]. The obtained pharmacokinetic results of this study will further guide the improvement of formulation development to enhance the quality attributes of Super-LbF.

Despite the advantages of superimposable pharmacokinetic profiles, maintaining the physical stability of super-LbF presents a significant challenge. This is primarily due to the inherent high chemical potential associated with the supersaturated state, which drives the system towards achieving a more favorable energy state through spontaneous re-crystallization [21]. To address this issue, precipitation inhibitors can be used in future studies to improve the stability of super-LbF by inhibiting drug nucleation and crystal growth in the liquid super-LbF [27]. These inhibitors may act through different mechanisms, including viscosity enhancement, increased drug solubility within the liquid LbF matrix, and facilitating favorable intermolecular interactions [7]. These precipitation inhibitors also can help to stabilize the *in-situ* supersaturation which is generated after dispersing the super-LbF in the aqueous media [18, 50, 51]. Formulation strategies such as the incorporation of solidifying lipids, or adsorption on solid carriers, could serve as potential approaches to sustain drug supersaturation for extended periods [16, 29]. In our study, we observed the need for advanced *in vitro* tools, such as a combined lipolysis-permeation setup, to improve the correlation between *in vitro* and *in vivo* outcomes. This setup could be employed to achieve better predictive accuracy for super-LbF. Our research group has been working in the same direction, to establish super-LbF as a viable formulation technique for use in preclinical, clinical, and manufacturing stages. From a pre-clinical perspective, super-LbF provided flexibility in the dose escalation studies, as well as simplicity of preparation and dosage loading. This makes them useful for simplified formulations from bench to clinic. Additionally, they save the effort required to bridge preclinical and clinical formulation types and provide for more flexibility in delivering dosage ranges during clinical studies. From a commercial manufacturing perspective, the production process of super-LbF is expected to be achievable through established simple industrial methods (solution mixing and heating).

Conclusion

In summary, the limited drug loading capacity of LbF presents a significant challenge in achieving the desired dose for pre-clinical or clinical studies. In the present study, the influence of the temperature-induced supersaturation method was investigated to enhance the solubility of Ibr and Enz within lipid solutions. The results indicate a significant improvement in drug loading capacity compared to conventional LbF, with a 2.5-fold increase for both Ibr and Enz.

However, the enhanced drug loading capacity comes with the trade-off of decreased physical stability over an extended period, leading to a risk of drug re-crystallization. The physical instability is influenced by the physicochemical properties of the drug and achieved aDS value. Also, super-LbF demonstrates significant changes in dispersion parameters, including droplet size and zeta potential. Additionally, we conducted a biopharmaceutical assessment to investigate the interplay between drug payload and *in-situ* supersaturation, followed by pharmacokinetic evaluations. During lipolysis studies, both conventional and super-LbF showed the generation of *in-situ* supersaturation for a shorter time period, subsequently posing a risk of drug precipitation. Furthermore, *in vivo* studies suggest that both conventional and super-LbF formulations exhibit comparable dose-normalized pharmacokinetic profiles. However, the *in vivo* performance of super-LbF suggests that maintaining a balance of supersaturation in the intestinal region is a pivotal factor. This can be improved by formulation interventions such as the use of precipitation inhibitors (PIs), controlling lipid digestion, and solidifying super-LbF. Overall, these findings may guide the improvement of formulation development to enhance the quality attributes of super-LbF.

Abbreviations aDS: Apparent degree of supersaturation; AUC : Area under the curve; 4-BPB: 4-Bromophenylboronic acid; Enz: Enzalutamide; Seq: Equilibrium solubility; GIT: Gastrointestinal tract; Ibr: Ibrutinib; LbF: Lipid-based formulation; LC: Long-chain; MC: Medium-chain; PDI: Polydispersity index; PWSD: Poorly water-soluble drug; PXRD: Powder X-ray diffraction:; SEDDS: Self-emulsifying drug delivery systems; Super-LbF: Supersaturated LbF; super-SNEDDS : Supersaturated self nano-emulsifying drug delivery systems; SR: Supersaturation ratio

Supplementary Information The online version contains supplementary material available at https://doi.org/10.1208/s12249-024-02912-9.

Acknowledgements The authors wish to acknowledge the Director of NIPER S.A.S. Nagar for providing the essential facilities and infrastructure for conducting the experimental work. The authors are also thankful to Mr. Ajay Lale for his assistance in manuscript proofreading.

Author Contributions Arvind Sirvi: Conceptualization, methodology, investigation, data curation, validation, manuscript writing and reviewing. Akash Janjal: Methodology, formal data analysis, manuscript reviewing and editing. Kajal Guleria: Formal data analysis, manuscript reviewing and editing. Mahesh Chand:Methodology (Pharmacokinetic study). Abhay T. Sangamwar: Conceptualization, data review, supervision, validation, project administration, writing-review and editing.

Funding Not applicable.

Data Availability Data will be made available on request.

Declarations

Ethics Approval All aspects of animal handling, care, and experimentation adhere to the ARRIVE guidelines and comply with the UK Animals (Scientific Procedures) Act, 1986, along with associated guidelines and the EU Directive 2010/63/EU for animal experiments. The protocol necessary for conducting a pharmacokinetic study on laboratory animals received approval from the Institutional Animal Ethics Committee, NIPER S.A.S. Nagar, India.

Conflict of Interest The authors declare that they have no conflict of interest.

References

1. Nadin A, Hattotuwagama C, Churcher I. Lead-oriented synthesis: a new opportunity for synthetic chemistry. Angew Chem Int Ed. 2012;51:1114–22. https://doi.org/10.1002/anie.201105840.
2. Stegemann S, Moreton C, Svanbäck S, Box K, Motte G, Paudel A. Trends in oral small-molecule drug discovery and product development based on product launches before and after the Rule of Five. Drug Discovery Today. 2023;28: 103344. https://doi.org/10.1016/j.drudis.2022.103344.
3. Feeney OM, Crum MF, McEvoy CL, Trevaskis NL, Williams HD, Pouton CW, Charman WN, Bergström CAS, Porter CJH. 50 years of oral lipid-based formulations: Provenance, progress and future perspectives. Adv Drug Deliv Rev. 2016;101:167–94. https://doi.org/10.1016/j.addr.2016.04.007.
4. Williams HD, Trevaskis NL, Yeap YY, Anby MU, Pouton CW, Porter CJH. Lipid-Based Formulations and Drug Supersaturation: Harnessing the Unique Benefits of the Lipid Digestion/Absorption Pathway. Pharm Res. 2013;30:2976–92. https://doi.org/10.1007/s11095-013-1126-0.
5. Sirvi A, Debaje S, Guleria K, Sangamwar AT. Critical aspects involved in lipid dispersion and digestion: Emphasis on in vitro models and factors influencing lipolysis of oral lipid based formulations. Adv Coll Interface Sci. 2023;321: 103028. https://doi.org/10.1016/j.cis.2023.103028.
6. Alvebratt C, Dening TJ, Åhlén M, Cheung O, Strømme M, Gogoll A, Prestidge CA, Bergström CAS. In Vitro Performance and Chemical Stability of Lipid-Based Formulations Encapsulated in a Mesoporous Magnesium Carbonate Carrier. Pharmaceutics. 2020;12:426. https://doi.org/10.3390/pharmaceutics12050426.
7. Holm R, Kuentz M, Ilie-Spiridon A-R, Griffin BT. Lipid based formulations as supersaturating oral delivery systems: From current to future industrial applications. Eur J Pharm Sci. 2023;189: 106556. https://doi.org/10.1016/j.ejps.2023.106556.
8. Koehl NJ, Henze LJ, Kuentz M, Holm R, Griffin BT. Supersaturated Lipid-Based Formulations to Enhance the Oral Bioavailability of Venetoclax. Pharmaceutics. 2020;12:564. https://doi.org/10.3390/pharmaceutics12060564.
9. Ilie A-R, Griffin BT, Brandl M, Bauer-Brandl A, Jacobsen A-C, Vertzoni M, Kuentz M, Kolakovic R, Holm R. Exploring impact of supersaturated lipid-based drug delivery systems of celecoxib on in vitro permeation across Permeapad® membrane and in vivo absorption. Eur J Pharm Sci. 2020;152: 105452. https://doi.org/10.1016/j.ejps.2020.105452.
10. Thomas N, Holm R, Müllertz A, Rades T. In vitro and in vivo performance of novel supersaturated self-nanoemulsifying drug delivery systems (super-SNEDDS). J Control Release. 2012;160:25–32. https://doi.org/10.1016/j.jconrel.2012.02.027.
11. Nora G-I, Venkatasubramanian R, Strindberg S, Siqueira-Jørgensen SD, Pagano L, Romanski FS, Swarnakar NK, Rades T, Müllertz A. Combining lipid based drug delivery and amorphous solid dispersions for improved oral drug absorption of a poorly water-soluble drug. J Control Release. 2022;349:206–12. https://doi.org/10.1016/j.jconrel.2022.06.057.
12. Panbachi S, Beranek J, Kuentz M. Hydrophobic deep eutectic solvent (HDES) as oil phase in lipid-based drug formulations. Int J

Pharm. 2024;661: 124418. https://doi.org/10.1016/j.ijpharm.2024.124418.
13. Jadhav K, Sirvi A, Janjal A, Kashyap MC, Sangamwar AT. Utilization of Lipophilic Salt and Phospholipid Complex in Lipid-Based Formulations to Modulate Drug Loading and Oral Bioavailability of Pazopanib. AAPS PharmSciTech. 2024;25:59. https://doi.org/10.1208/s12249-024-02780-3.
14. Sirvi A, Jadhav K, Sangamwar AT. Enabling superior drug loading in lipid-based formulations with lipophilic salts for a brick dust molecule: Exploration of lipophilic counterions and in vitro-in vivo evaluation. Int J Pharm. 2024;656:124108. https://doi.org/10.1016/j.ijpharm.2024.124108.
15. Bennett-Lenane H, O'Shea JP, Murray JD, Ilie A-R, Holm R, Kuentz M, Griffin BT. Artificial Neural Networks to Predict the Apparent Degree of Supersaturation in Supersaturated Lipid-Based Formulations: A Pilot Study. Pharmaceutics. 2021;13:1398. https://doi.org/10.3390/pharmaceutics13091398.
16. Schultz HB, Thomas N, Rao S, Prestidge CA. Supersaturated silica-lipid hybrids (super-SLH): An improved solid-state lipid-based oral drug delivery system with enhanced drug loading. Eur J Pharm Biopharm. 2018;125:13–20. https://doi.org/10.1016/j.ejpb.2017.12.012.
17. Almasri R, Joyce P, Schultz HB, Thomas N, Bremmell KE, Prestidge CA. Prestidge, Porous Nanostructure, Lipid Composition, and Degree of Drug Supersaturation Modulate In Vitro Fenofibrate Solubilization in Silica-Lipid Hybrids. Pharmaceutics. 2020;12:687. https://doi.org/10.3390/pharmaceutics12070687.
18. Bannow J, Yorulmaz Y, Löbmann K, Müllertz A, Rades T. Improving the drug load and in vitro performance of supersaturated self-nanoemulsifying drug delivery systems (super-SNEDDS) using polymeric precipitation inhibitors. Int J Pharm. 2020;575: 118960. https://doi.org/10.1016/j.ijpharm.2019.118960.
19. Ilie A-R, Griffin BT, Kolakovic R, Vertzoni M, Kuentz M, Holm R. Supersaturated lipid-based drug delivery systems – exploring impact of lipid composition type and drug properties on supersaturability and physical stability. Drug Dev Ind Pharm. 2020;46:356–64. https://doi.org/10.1080/03639045.2020.1721526.
20. Siqueira SDVS, Müllertz A, Gräeser K, Kasten G, Mu H, Rades T. Influence of drug load and physical form of cinnarizine in new SNEDDS dosing regimens: in vivo and in vitro evaluations. AAPS J. 2017;19:587–94. https://doi.org/10.1208/s12248-016-0038-4.
21. Paulus F, Bauer-Brandl A, Stappaerts J, Holm R. Digestion is a critical element for absorption of cinnarizine from supersaturated lipid-based type I formulations. Eur J Pharm Sci. 2024;192: 106634. https://doi.org/10.1016/j.ejps.2023.106634.
22. Paulus F, Holm R, Stappaerts J, Bauer-Brandl A. Absorption of cinnarizine from type II lipid-based formulations: Impact of lipid chain length, supersaturation, digestion, and precipitation inhibition. Eur J Pharm Sci. 2024;197: 106765. https://doi.org/10.1016/j.ejps.2024.106765.
23. Wilson V, Lou X, Osterling DJ, Stolarik DF, Jenkins G, Gao W, Zhang GGZ, Taylor LS. Relationship between amorphous solid dispersion in vivo absorption and in vitro dissolution: phase behavior during dissolution, speciation, and membrane mass transport. J Control Release. 2018;292:172–82. https://doi.org/10.1016/j.jconrel.2018.11.003.
24. Ohtsu Y, Gibbons JA, Suzuki K, Fitzsimmons ME, Nozawa K, Arai H. Absorption, Distribution, Metabolism, and Excretion of the Androgen Receptor Inhibitor Enzalutamide in Rats and Dogs. Eur J Drug Metab Pharmacokinet. 2017;42:611–26. https://doi.org/10.1007/s13318-016-0374-x.
25. Stewart AM, Grass ME. Practical approach to modeling the impact of amorphous drug nanoparticles on the oral absorption of poorly soluble drugs. Mol Pharmaceutics. 2020;17:180–9. https://doi.org/10.1021/acs.molpharmaceut.9b00889.
26. Matsumura N, Ono A, Akiyama Y, Fujita T, Sugano K. Bottom-up physiologically based oral absorption modeling of free weak base drugs. Pharmaceutics. 2020;12:844. https://doi.org/10.3390/pharmaceutics12090844.
27. Sirvi A, Kuche K, Chaudhari D, Ghadi R, Date T, Katiyar SS, Jain S. Supersaturable self-emulsifying drug delivery system: A strategy for improving the loading and oral bioavailability of quercetin. Journal of Drug Delivery Science and Technology. 2022;71: 103289. https://doi.org/10.1016/j.jddst.2022.103289.
28. Thomas N, Müllertz A, Graf A, Rades T. Influence of Lipid Composition and Drug Load on the In Vitro Performance of Self-Nanoemulsifying Drug Delivery Systems. J Pharm Sci. 2012;101:1721–31. https://doi.org/10.1002/jps.23054.
29. Mondal S, Sirvi A, Jadhav K, Sangamwar AT. Supersaturating lipid-based solid dispersion of atazanavir provides enhanced solubilization and supersaturation in the digestive aqueous phase. Int J Pharm. 2023;638: 122919. https://doi.org/10.1016/j.ijpharm.2023.122919.
30. Michaelsen MH, Siqueira Jørgensen SD, Abdi IM, Wasan KM, Rades T, Müllertz A. Fenofibrate oral absorption from SNEDDS and super-SNEDDS is not significantly affected by lipase inhibition in rats. Eur J Pharm Biopharm. 2019;142(2019):258–264. https://doi.org/10.1016/j.ejpb.2019.07.002.
31. Kilic M, Dressman J. A simplified method to screen for in-vivo performance of oral lipid formulations. J Pharm Pharmacol. 2014;66:615–23. https://doi.org/10.1111/jphp.12182.
32. Qiu Q, Lu M, Li C, Luo X, Liu X, Hu L, Liu M, Zheng H, Zhang H, Liu M, Lai C, Song Y, Deng Y. Novel Self-Assembled Ibrutinib-Phospholipid Complex for Potently Peroral Delivery of Poorly Soluble Drugs with pH-Dependent Solubility. AAPS PharmSciTech. 2018;19:3571–83. https://doi.org/10.1208/s12249-018-1147-4.
33. Fridgeirsdottir GA, Harris R, Fischer PM, Roberts CJ. Support Tools in Formulation Development for Poorly Soluble Drugs. J Pharm Sci. 2016;105:2260–9. https://doi.org/10.1016/j.xphs.2016.05.024.
34. Pouton CW. Formulation of poorly water-soluble drugs for oral administration: Physicochemical and physiological issues and the lipid formulation classification system. Eur J Pharm Sci. 2006;29:278–87. https://doi.org/10.1016/j.ejps.2006.04.016.
35. Brinkmann J, Huxoll F, Luebbert C, Sadowski G. Solubility of pharmaceutical ingredients in triglycerides. Eur J Pharm Biopharm. 2019;145:113–20. https://doi.org/10.1016/j.ejpb.2019.10.012.
36. Lee S-M, Lee J-G, Yun T-H, Cho J-H, Kim K-S. Enhanced Stability and Improved Oral Absorption of Enzalutamide with Self-Nanoemulsifying Drug Delivery System. Int J Mol Sci. 2024;25:1197. https://doi.org/10.3390/ijms25021197.
37. Suys EJA, Chalmers DK, Pouton CW, Porter CJH. Polymeric Precipitation Inhibitors Promote Fenofibrate Supersaturation and Enhance Drug Absorption from a Type IV Lipid-Based Formulation. Mol Pharmaceutics. 2018;15:2355–71. https://doi.org/10.1021/acs.molpharmaceut.8b00206.
38. Francke NM, Bunjes H. Influence of drug loading on the physical stability of phospholipid-stabilised colloidal lipid emulsions. Int J Pharm X. 2020;2: 100060. https://doi.org/10.1016/j.ijpx.2020.100060.
39. Anby MU, Williams HD, McIntosh M, Benameur H, Edwards GA, Pouton CW, Porter CJH. Lipid Digestion as a Trigger for Supersaturation: Evaluation of the Impact of Supersaturation Stabilization on the in Vitro and in Vivo Performance of Self-Emulsifying Drug Delivery Systems. Mol Pharmaceutics. 2012;9:2063–79. https://doi.org/10.1021/mp300164u.

40. Devraj R, Williams HD, Warren DB, Mohsin K, Porter CJH, Pouton CW. In vitro assessment of drug-free and fenofibrate-containing lipid formulations using dispersion and digestion testing gives detailed insights into the likely fate of formulations in the intestine. Eur J Pharm Sci. 2013;49:748–60. https://doi.org/10.1016/j.ejps.2013.04.036.
41. Crum MF, Trevaskis NL, Pouton CW, Porter CJH. Transient Supersaturation Supports Drug Absorption from Lipid-Based Formulations for Short Periods of Time, but Ongoing Solubilization Is Required for Longer Absorption Periods. Mol Pharmaceutics. 2017;14:394–405. https://doi.org/10.1021/acs.molpharmaceut.6b00792.
42. Suys EJA, Brundel DHS, Chalmers DK, Pouton CW, Porter CJH. Interaction with biliary and pancreatic fluids drives supersaturation and drug absorption from lipid-based formulations of low (saquinavir) and high (fenofibrate) permeability poorly soluble drugs. J Control Release. 2021;331:45–61. https://doi.org/10.1016/j.jconrel.2021.01.007.
43. Alskär LC, Keemink J, Johannesson J, Porter CJH, Bergström CAS. Impact of Drug Physicochemical Properties on Lipolysis-Triggered Drug Supersaturation and Precipitation from Lipid-Based Formulations. Mol Pharmaceutics. 2018;15:4733–44. https://doi.org/10.1021/acs.molpharmaceut.8b00699.
44. Sassene PJ, Knopp MM, Hesselkilde JZ, Koradia V, Larsen A, Rades T, Müllertz A. Precipitation of a Poorly Soluble Model Drug during In Vitro Lipolysis: Characterization and Dissolution of the Precipitate. J Pharm Sci. 2010;99:4982–91. https://doi.org/10.1002/jps.22226.
45. Lee KWY, Porter CJH, Boyd BJ. The Effect of Administered Dose of Lipid-Based Formulations on the In Vitro and In Vivo Performance of Cinnarizine as a Model Poorly Water-Soluble Drug. J Pharm Sci. 2013;102:565–78. https://doi.org/10.1002/jps.23384.
46. Stillhart C, Kuentz M. Trends in the Assessment of Drug Supersaturation and Precipitation In Vitro Using Lipid-Based Delivery Systems. J Pharm Sci. 2016;105:2468–76. https://doi.org/10.1016/j.xphs.2016.01.010.
47. Tanaka Y, Doi H, Katano T, Kasaoka S. The impact of quantity of lipid based formulations with different compositions on the oral absorption of ritonavir: A trade-off between apparent solubility and permeability. Eur J Pharm Sci. 2022;168: 106079. https://doi.org/10.1016/j.ejps.2021.106079.
48. Thomas N, Richter K, Pedersen TB, Holm R, Müllertz A, Rades T. In vitro lipolysis data does not adequately predict the in vivo performance of lipid-based drug delivery systems containing fenofibrate. AAPS J. 2014;16:539–49. https://doi.org/10.1208/s12248-014-9589-4.
49. Siqueira Jørgensen SD, Al Sawaf M, Graeser K, Mu H, Müllertz A, Rades T. The ability of two in vitro lipolysis models reflecting the human and rat gastro-intestinal conditions to predict the in vivo performance of SNEDDS dosing regimens. Eur J Pharm Biopharm. 2018;2018(124):116–24. https://doi.org/10.1016/j.ejpb.2017.12.014.
50. Koehl NJ, Henze LJ, Bennett-Lenane H, Faisal W, Price DJ, Holm R, Kuentz M, Griffin BT. In Silico, In Vitro, and In Vivo Evaluation of Precipitation Inhibitors in Supersaturated Lipid-Based Formulations of Venetoclax. Mol Pharmaceutics. 2021;18:2174–88. https://doi.org/10.1021/acs.molpharmaceut.0c00645.
51. Ilie A-R, Griffin BT, Vertzoni M, Kuentz M, Kolakovic R, Prudic-Paus A, Malash A, Bohets H, Herman J, Holm R. Exploring precipitation inhibitors to improve in vivo absorption of cinnarizine from supersaturated lipid-based drug delivery systems. Eur J Pharm Sci. 2021;159:105691. https://doi.org/10.1016/j.ejps.2020.105691.